CHAPTER IV
RESULTS AND DISCUSSION

In this chapter, the methyl ester and alpha methyl ester sulfonate characterization results are discussed in Section 4.1. The influences of the different reactant and initiator systems, and reaction time of the suitable system are analyzed and discussed in Sections 4.2 and 4.3, respectively. The reaction was performed in a photochemical reactor consisting of 16 lamps (253.7 nm) at 40 °C under atmospheric pressure.

4.1 Characterization of Palm Oil Methyl Ester and Alpha Methyl Ester Sulfonates C16 and 18

This section discusses about the characterization of methyl ester (ME) and alpha methyl ester sulfonate C16 and 18 (α-MES C16 and C18) by using several characterization techniques. Functional groups of samples were analyzed by Fourier Transform Infrared Spectroscopy (FT-IR). The carbon distribution of methyl ester was determined by Gas Chromatography-Mass spectrometry (GC-MS). The ions of m/z in negative mode of α-MES were analyzed by Electrospray Ionization Mass Spectrometry (ESI-MS).

4.1.1 Characterization of Palm Oil Methyl Ester

The Infrared spectrum of palm oil methyl ester was investigated. IR spectrum is plotted in Figure 4.1. The IR spectrum shows the typical frequencies of linear alkane and carbonyl groups. As the palm oil methyl ester is mainly monoalkyl ester, the high intensity of -C-O and -C=O band of ester appears at 1,170 and 1,742 cm^{-1}, respectively. Moreover, $-CH_2-$ symmetric and asymmetric stretching frequencies of linear alkane show two peak ranging from 2,852 to 2,929 cm^{-1}, while $-CH_2-$ bending frequency appears at 1,460 cm^{-1} (Imahara *et al.*, 2008).

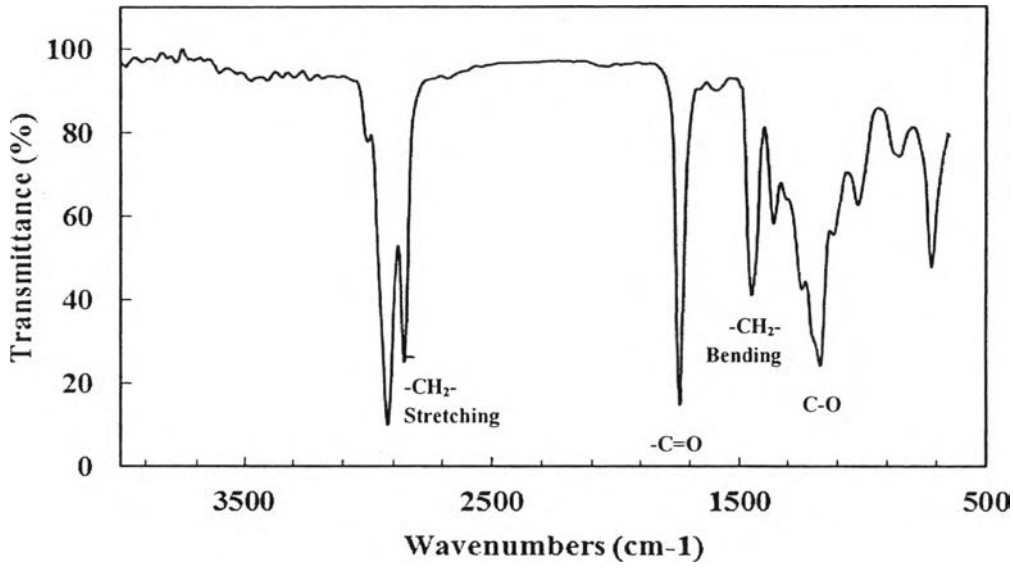

Figure 4.1 Infrared spectrum of palm oil methyl ester (ME).

Gas chromatographic-mass spectrometry (GC-MS) was used to find the carbon distribution of palm oil methyl ester as shown in Figure 4.2. The distribution and composition of each component are concluded in Table 4.1. Methyl ester used in this experiment consists of 36.0 % C16 and 64.0 % C18.

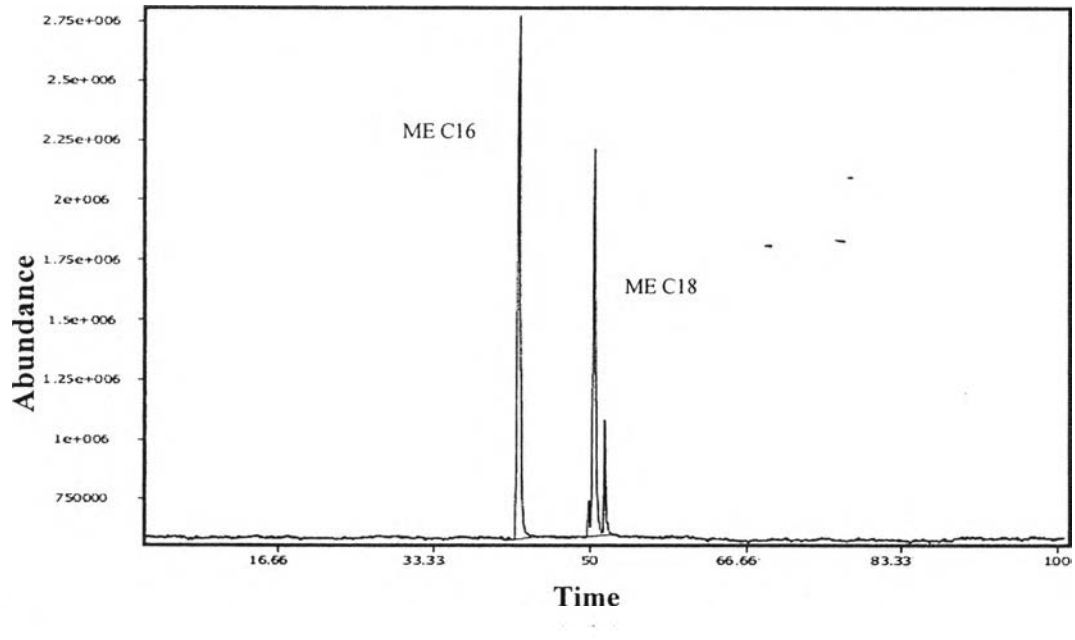

Figure 4.2 Total ion chromatogram (TIC) of palm oil methyl ester.

Table 4.1 Fatty acid composition in palm oil methyl ester

Fatty acid		Formula	Molecular weight	Area (% mol)
Palmitic acid methyl ester	C16:0	$C_{17}H_{34}O_2$	270	36.0
Octadecenoic acid methyl ester	C18:1	$C_{19}H_{36}O_2$	296	45.4
Linoleic acid methyl ester	C18:2	$C_{19}H_{34}O_2$	294	0.5
Stearic acid methyl ester	C18:3	$C_{19}H_{38}O_2$	298	18.1

4.1.2 Characterization of Alpha Methyl Ester Sulfonates C16 and 18

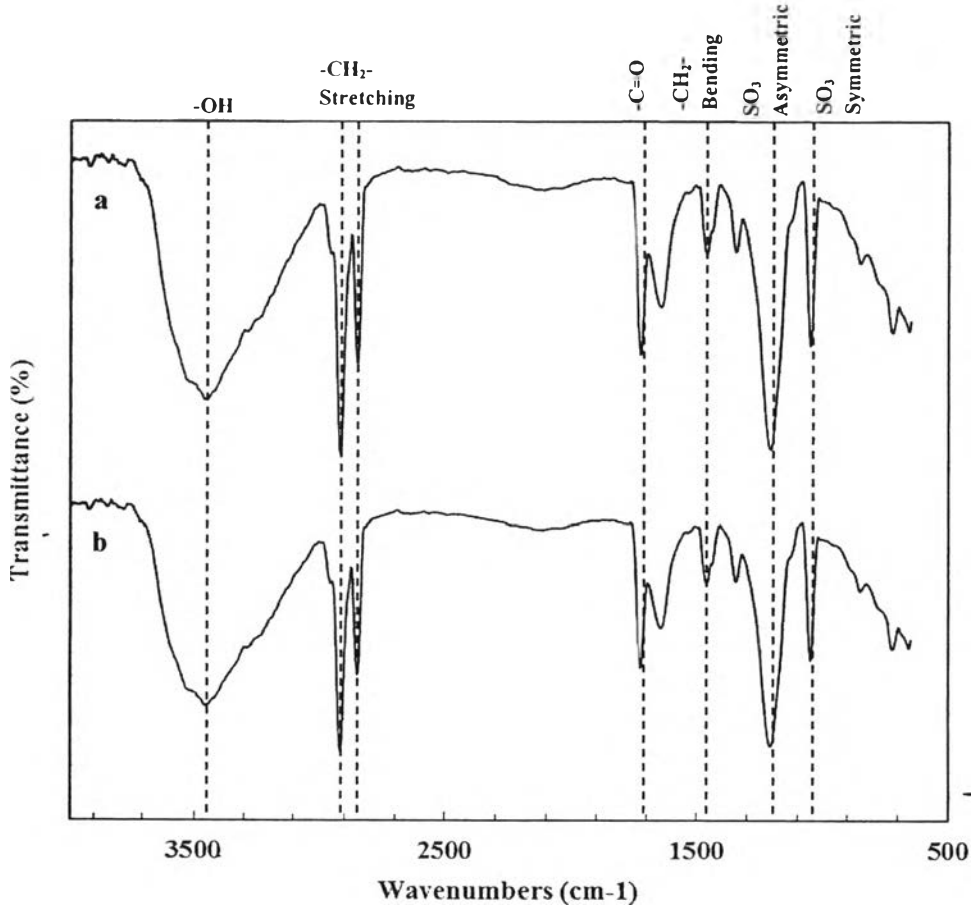

Figure 4.3 Infrared spectra of (a) α-MES C16 and (b) α-MES C18.

The IR spectra of α-MES C16 and 18 are shown in Figure 4.3 and concluded in Table 4.2. The board IR peak of hydroxyl group results from water presenting at 3,429 cm^{-1}. Strong peaks around 2,850-2,930 cm^{-1} corresponds to CH_2-symmetric and asymmetric stretching frequencies. The bands at 1,046 and 1,210 cm^{-1}

indicate the presence of sulfonate symmetric and asymmetric stretching frequencies, respectively (Cohen *et al.*, 1998, Elraies *et al.*, 2010).

The ESI-MS fingerprints of α-MES C16 and 18 observed in the negative mode fingerprints are shown in Figure 4.4 and 4.5, respectively. For the fingerprints of α-MES C16, the ion of m/z 349 is obviously appeared, whereas α-MES C18 shows the ions of m/z 377 which is the most intense in the sample.

Table 4.2 The main IR peaks and the corresponding functional groups of α-MES C16 and 18

Peak (cm^{-1})	Functional groups
3,429	OH stretching frequency
1,725	-C=O stretching frequency of ester
2,850-2,930	CH_2- symmetric and asymmetric stretching frequency
1,467	CH_2- bending frequency
1,210	SO_3 asymmetric stretching frequency
1,046	SO_3 symmetric stretching frequency in R-SO_3

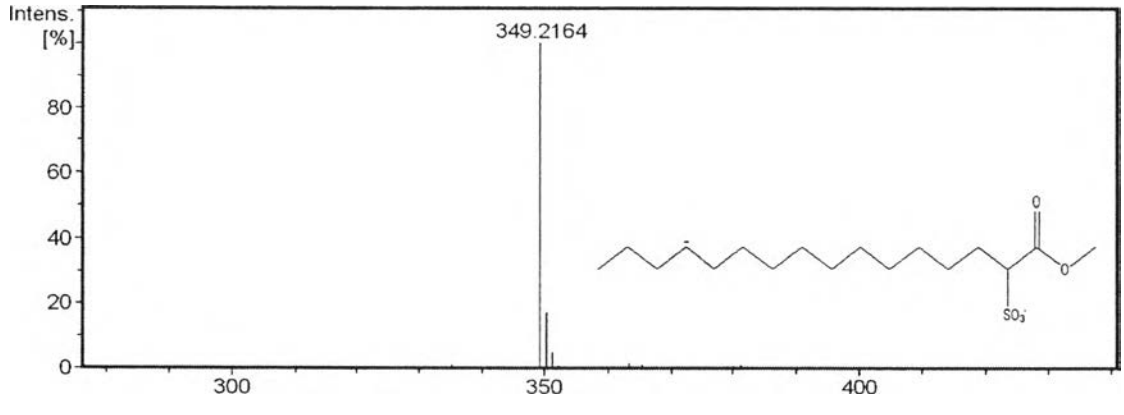

Figure 4.4 ESI-MS fingerprints of α-MES C16.

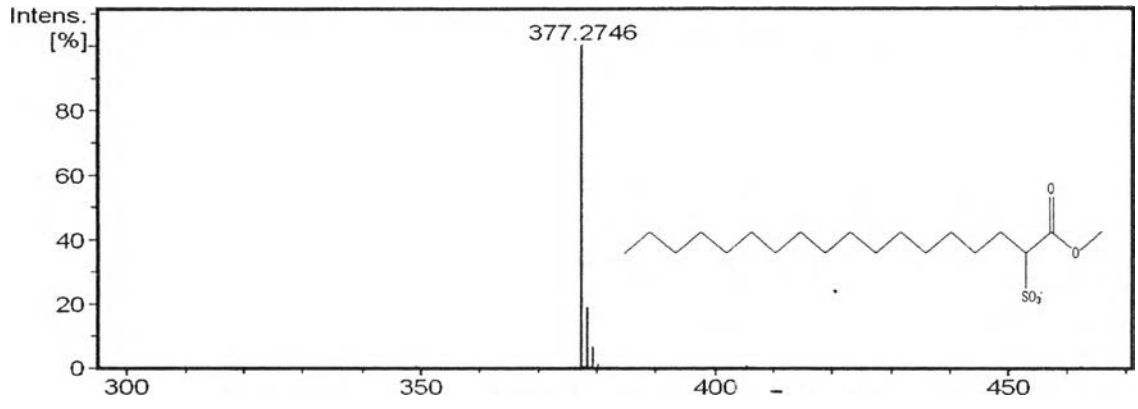

Figure 4.5 ESI-MS fingerprints of α-MES C18.

4.2 Effect of Different Reactants and Initiators

This section discusses about the investigation of the presence of different reactants and initiators in order to convert methyl ester to methyl ester sulfonate. There are four systems as follows: UV/O_2, O_3/O_2, $UV/O_3/O_2$, and UV/O_3. In this case, flow rate of SO_2 and O_2 were fixed at 100 ml/min, whereas O_3 was at 0.5 l/min (Table 4.3). The reaction was performed at 40 °C under atmospheric pressure for 4 hours.

Table 4.3 Experimental design for studying the effect of different reactants and initiators

System	Experimental Set				Reaction time (hr)	Abbreviation
	Initiator		Reactant			
	UV	O_3 (l/min)	SO_2 (ml/min)	O_2 (ml/min)		
1	YES	0	100	100	4	UV/O_2
2	NO	0.5	100	100	4	O_3/O_2
3	YES	0.5	100	100	4	$UV/O_3/O_2$
4	YES	0.5	100	0	4	UV/O_3

4.2.1 Conversion Calculation

After an upper layer in a separatory funnel was transferred to a rotary evaporator, the small amount of water was separated out, and then unreacted methyl ester was weighed to calculate conversion. Conversion percentages are reported in Table 4.4. The first and second systems were studied so as to investigate the effect of different initiators. UV light and O_3 are individually used as an initiator for the first and second systems, respectively. The conversion of these two systems is 7.5 %w/w and 6.9 %w/w, which are not significantly different. However, when UV light and O_3 are used together in the third system, conversion increases up to approximately 13.5 %w/w, which is improved by 6.0 %w/w and 6.6 %w/w for the first and second systems, respectively. In addition, the effect of the presence of O_2 was studied in the third and fourth systems. It ean be noticed that when O_2 is not fed into the system, conversion dramatically drops from 13.5 %w/w to 3.6 %w/w. This can be concluded that oxygen plays an important role in generating sulfonate groups. According to Eq. 2.14, O_2 collides with $RSO_2^{\cdot}$ in order to form $RSO_2OO^{\cdot}$, which further react and become RSO_3H as a desired product (Ramakrishnan, 2006). Therefore, O_2 is one of the main factors for synthesizing MES.

Table 4.4 Conversion of each system

	Systems	Conversion (%w/w)
1	UV/O_2	7.5
2	O_3/O_2	6.9
3	$UV/O_3/O_2$	13.5
4	UV/O_3	3.6

4.2.2 Characterization of Products

4.2.2.1 Fourier Transform Infrared Spectroscopy

When reaction was done, product outlets were mixed with hot water in order to separate desired products into a water phase and left only unreacted methyl ester in an upper phase. Unreacted methyl ester of all systems was investigated by FT-IR in order to compare with palm oil methyl ester.

From Figure 4.6, the spectra of unreacted methyl ester from four systems (b - e) show mostly the same functional groups as palm oil methyl ester. However, it can be clearly seen that there are two separated peaks at~1,700 – 1,725 cm^{-1} in unreacted methyl ester. The first peak at~1,725 cm^{-1} refers to a carbonyl group of ester, whereas the other at~1,710 cm^{-1} represents a carbonyl of saturated carboxylic acids (Amornsit *et al.*, 1991). In addition, the low and broad band around 2,500 – 3,500 cm^{-1}, which overlap with the C-H region, represents O-H single bond stretching band of carboxylic acid (Soderberg, 2014). The cause of carboxylic acid may be due to methyl ester groups are hydrolyzed by water to become carboxylic groups. Nevertheless, carboxylic groups of fatty acids can be recovered by esterification with a large excess of anhydrous methanol and an acidic reagent as catalyst as shown in Eq. 4.1 (Prateepchaikul *et al.*, 2007). As a result, unreacted methyl ester can be reused.

$$RCOOH + CH_3OH \xrightleftharpoons{H^+} RCOOCH_3 + H_2O \qquad \text{Eq. 4.1}$$

Regarding the aqueous phase, after separation and purification steps, liquid samples were neutralized with 30 %w/w NaOH and were tested by FT-IR. Figure 4.7 shows the IR spectra of α-MES C18 compared to those of synthesized MES from four systems. It is found that all synthesized MES samples show the same frequencies as α-MES C18, which are 3,456 cm^{-1} (OH stretching), 2,859-2,928 cm^{-1} (-CH_2- symmetric and asymmetric stretching), 1,742 cm^{-1} (-C=O stretching of ester), 1,457 cm^{-1} (-CH_2- bending), 1,200 cm^{-1} (SO_3 asymmetric stretching), and 1,040 cm^{-1} (SO_3 symmetric stretching in R-SO_3). This can be used to confirm that MES products are successfully sulfonated via the sulfoxidation reaction.

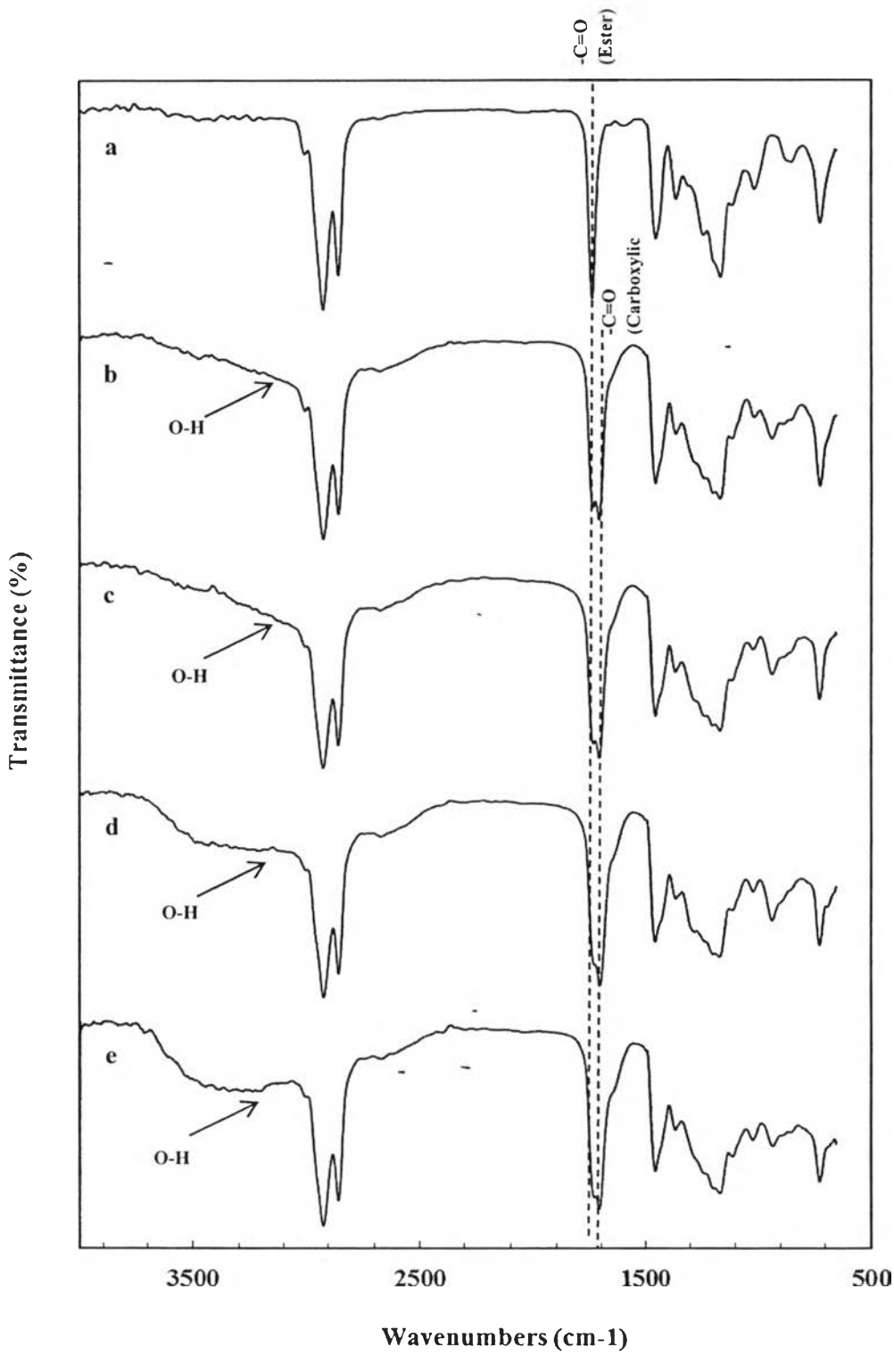

Figure 4.6 Infrared spectra of a) ME compared to unreacted ME from different systems b) UV/O_2 c) O_3/O_2 d) $UV/O_3/O_2$ e) UV/O_3.

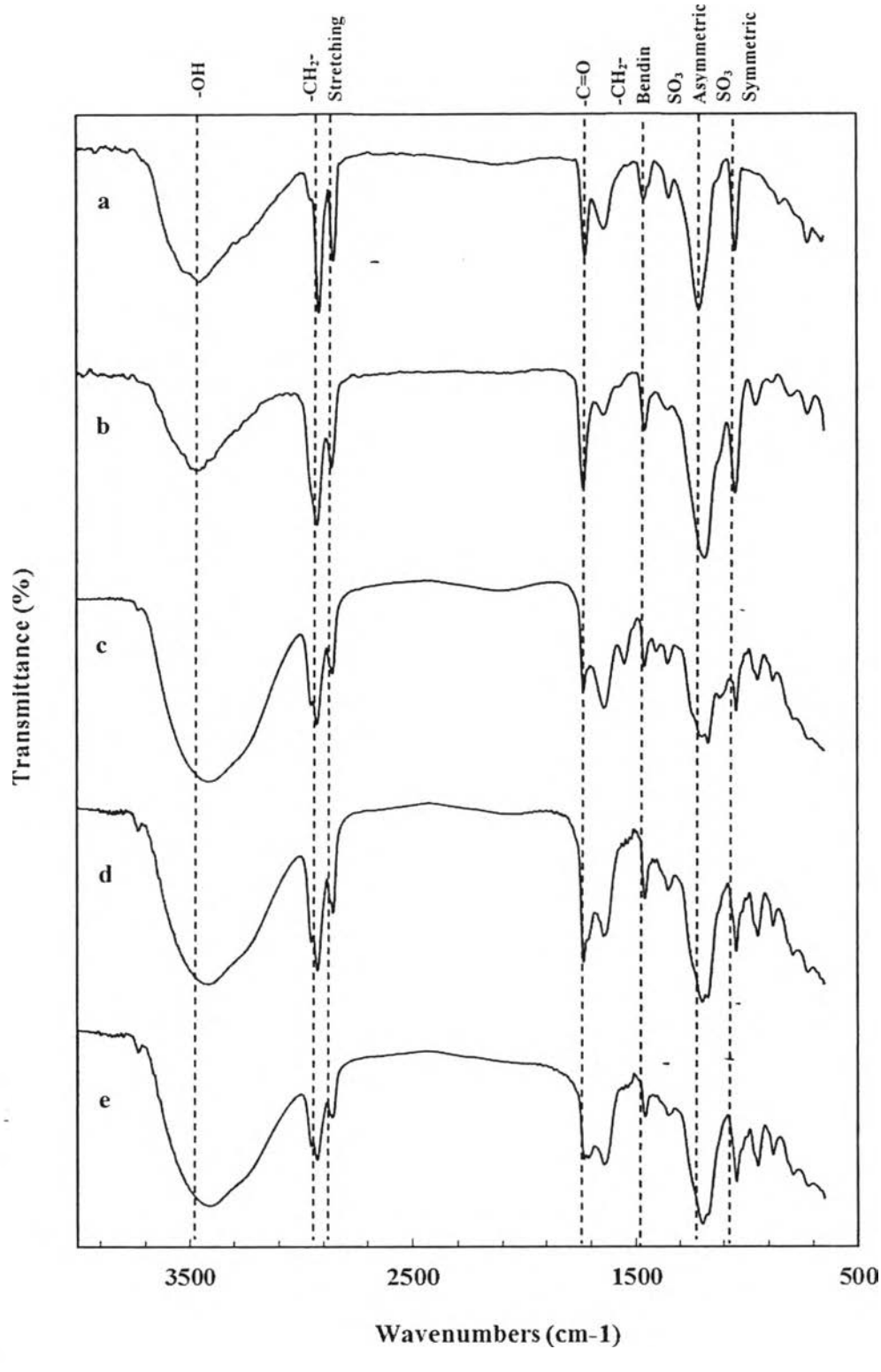

Figure 4.7 Infrared spectrum of a) alpha MES C18 compared to neutralized MES from different systems b) UV/O_2 c) O_3/O_2 d) $UV/O_3/O_2$ e) UV/O_3.

4.2.2.2 Gas Chromatography-Mass Spectrometry

GC-MS was used to carry out the relative sulfonatability of different homologs (C16 and C18). As mention before, starting methyl ester consists of C16 and C18. When methyl ester was sulfoxidized, the composition of unreacted methyl ester was changed as shown in Table 4.5. The results show that a small amount of C12 and C14 methyl ester is occurred after the reaction is finished. The cause of a small amount of shorter carbon chains may come from two reasons. The first reason is due to ozonolysis at double bonds of methyl ester (Soriano Jr *et al.*, 2003). The second reason is photolysis, which is a chemical process that molecule are broken down into smaller units through the absorption of light. In this case, UV carries enough energy to break carbon-carbon bonds since UVC at wavelength of 253.7 nm contains about 4.9 eV (Havinga, 1991), which is higher than the energy of a carbon-carbon bond (3.6 eV) (Luo, 2002). As a consequence, UV can decompose this single carbon-carbon bond to become shorter carbon chain. In addition, it can be seen that the relative content of C18 starting ME is less than that of C18 unreacted ME in all systems (1 - 4). On the other hand, the relative content of C16 unreacted ME for all systems increases compared to that of C16 starting ME. It means that the sulfonatability of the C18 ME is higher than that of C16 ME. This is because C18 ME have a longer carbon chain which provides more probability for gaseous reactants (SO_2, O_2, and O_3) to collide with carbon chain (Cohen *et al.*, 2006).

Table 4.5 Sulfonatability of methyl ester and unreacted methyl ester

Carbon Chain Length of Methyl ester	Starting Methyl Ester (% mol)	Unreacted Methyl ester of each System (%mol)			
		1) UV/O_2	2) O_3/O_2	3) $UV/O_3/O_2$	4) UV/O_3
C12	0.0	0.5	1.1	1.2	3.3
C14	0.0	4.6	7.0	8.0	11.8
C16	36.0	46.8	45.1	43.0	48.7
C18	64.0	48.1	46.8	47.8	36.1

4.2.2.3 Electrospray Ionization Mass Spectrometry

MES products were analyzed by direct infusion negative ion mode electrospray ionization mass spectrometry (ESI-MS). All fingerprints (Figure 4.9 (a – d)) display ions of m/z 361, 379, 393, 443, 459, 473, and 491 with various intensities. The ions of m/z 361, 379, and 393 represent monosulfonates of C18, whereas 443, 459, 473, and 491 refer to disulfonates of C18. According to the sufoxidation mechanism in Eq 2.11-2.10, there are many intermediates happening during the reaction, such as $RSO_2^{\cdot}$, $RSO_3^{\cdot}$, and $RSO_4^{\cdot}$. It can be noted that the three large peaks at 361, 379, and 393 mass units correspond to monosulfonates in the forms of RSO_2H, RSO_3H, and RSO_4H, respectively. Furthermore, the four peaks having the masses 443, 459, 473, and 491 represent disulfonates. The first peak at 443 refers to C18 having $-SO_2H$ and $-SO_3H$. The second peak at 459 refers to C18 having two groups of $-SO_3H$. The third peak at 473 refers to C18 having $-SO_3H$ and $-SO_4H$. Finally, the mass at 491 refers to C18 having two groups of $-SO_4H$. Figure 4.8 shows the possible structure of mono- and disulfonates presenting in MES products. The height of peaks does not reflect the abundance of the different sulfonated species. Therefore, the ESI results only indicate that there are both mono- and disulfonates in MES products.

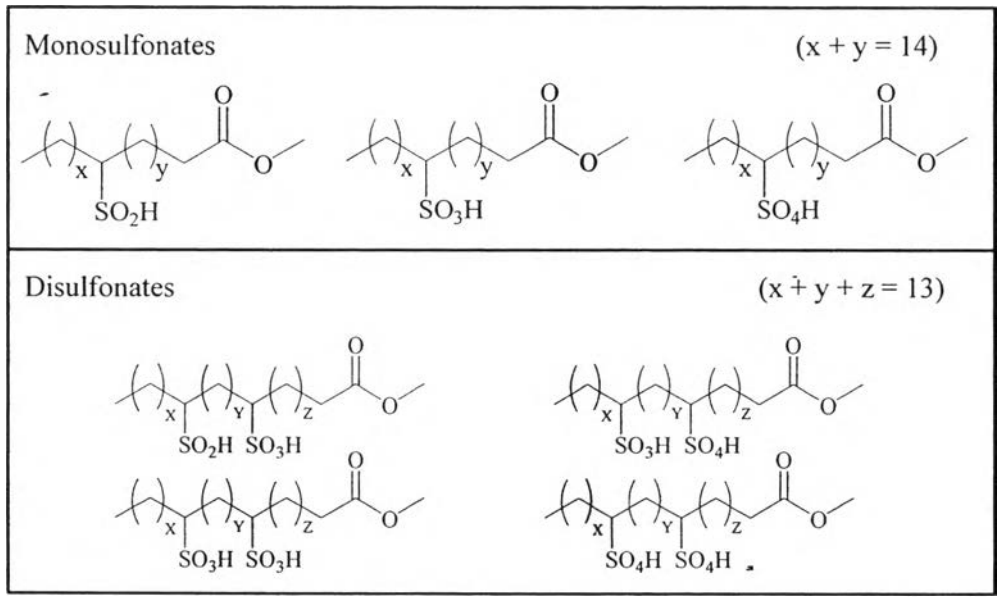

Figure 4.8 The possible structure of mono- and disulfonates in MES products.

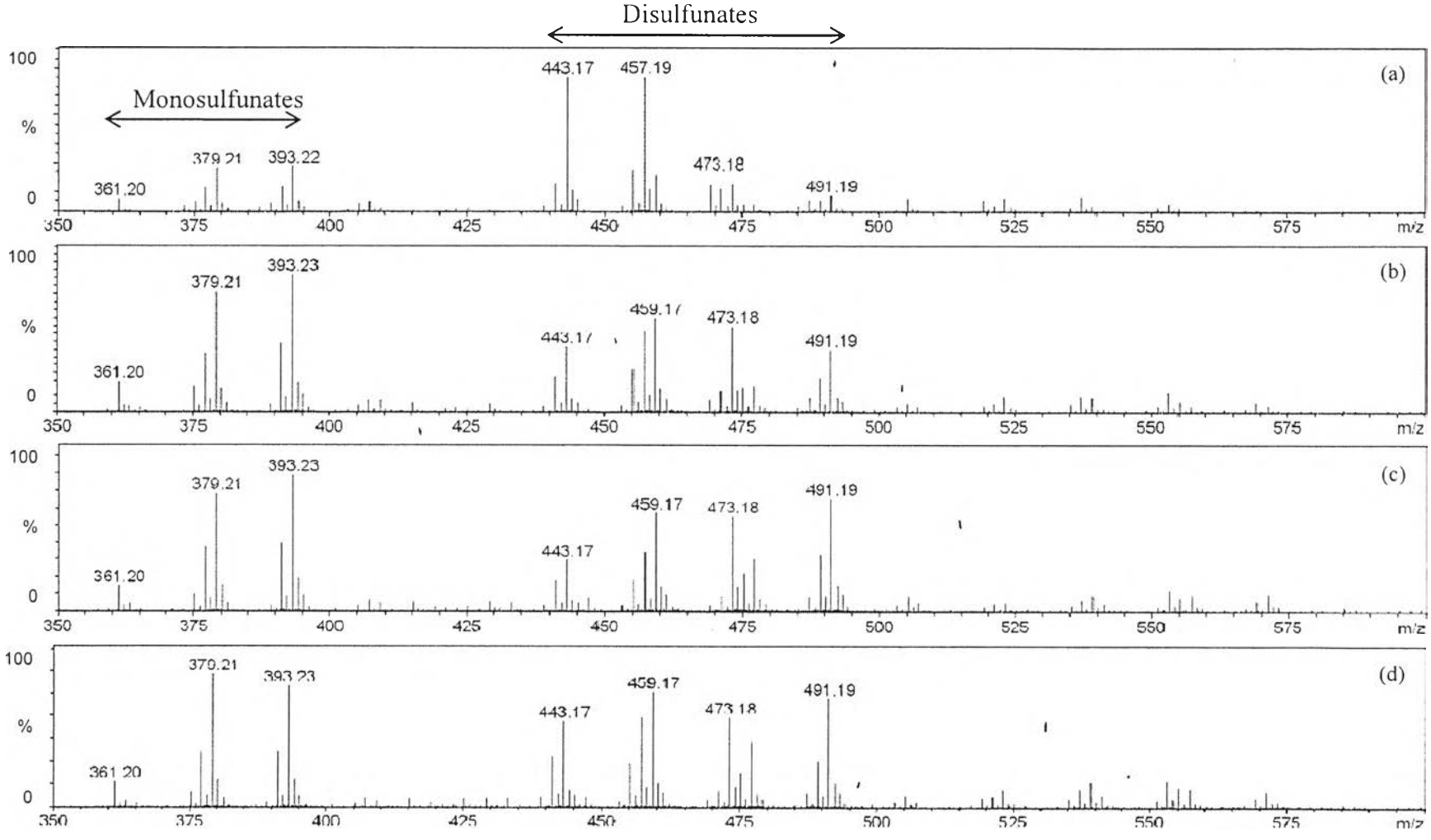

Figure 4.9 ESI-MS fingerprints in the negative ion mode of a) UV/O_2 b) O_3/O_2 c) $UV/O_3/O_2$ d) UV/O_3.

4.3 Effect of Reaction Time

This section discusses about the influence of increasing reactant reaction time. According to section 4.2, when both UV and O_3 were used as an initiator, it provides the highest conversion compared to using individual UV or O_3. Thus, the $UV/O_3/O_2$ system was used to study the effect of reaction time. Reaction time was 1, 2, 4, and 6 hours. The flow rates of SO_2 and O_2 were fixed at 100 ml/min, whereas that of O_3 was at 0.5 l/min. The reaction was performed at 40 °C. The experiment design and conditions for studying the effect of reaction is shown in Table 4.6.

Table 4.6 Experimental design for studying the effect of reaction time

System	Experimental Set				Reaction time (hr)	Abbreviation
	Initiator		Reactant			
	UV	O_3 (l/min)	SO_2 (ml/min)	O_2 (ml/min)		
5	YES	0.5	100	100	1	$1UV/O_3/O_2$
6	YES	0.5	100	100	2	$2UV/O_3/O_2$
7	YES	0.5	100	100	4	$4UV/O_3/O_2$
8	YES	0.5	100	100	6	$6UV/O_3/O_2$

4.3.1 Conversion Calculation

Conversion percentages and the total products are calculated and reported in Table 4.7. As expected, conversion and the weight of total products increase with reaction time. Conversion is approximately 4.7, 10.2, 13.5, and 14.7 %wt for 1, 2, 4, and 6 hours, respectively. In addition, the total MES products for 1, 2, 4, and 6 hours are about 5.9, 13.0, 17.5, and 20.8 g, respectively, when using 172 g (200 ml) of methyl ester in each batch.

Table 4.7 Conversion and weight of total products at 1, 2, 4, and 6 hrs

System	Reaction Time (hr)	Conversion (%w/w)	Total products (g)
$1UV/O_3/O_2$	1	4.7	5.9
$2UV/O_3/O_2$	2	10.2	13.0
$4UV/O_3/O_2$	4	13.5	17.5
$6UV/O_3/O_2$	6	14.7	20.8

4.3.2 Selectivity Calculation

For selectivity calculation, HPLC-UV was used to calculate peak areas of mono- and disulfonates. In this study, selectivity is the ratio of monosulfonates to disulfonates. Figure 4.10 shows chromatogram of α-MES C18, which presents one intense peak at 5.4 min. HPLC chromatograms of the $UV/O_3/O_2$ system at different reaction time are shown in Figure 4.10 - 4.14. ESI-MS fingerprints (Figure 4.15 and 4.16) are used to identify that the first peak at ~ 4.7 min represents disulfonates and the second peak at ~ 5.7 - 6.1 min refers to monosulfonates. It is found that the percent composition of monosulfonates increases, while percent composition of disulfonates increases. In other words, the ratios of monosulfonates to disulfonates slightly decline with the increase of reaction time as reported in Table 4.8 and plotted in Figure 4.17. The selectivity of each system is roughly 11.7, 10.9, 7.9, and 5.3 for 1, 2, 4, and 6 hours, respectively.

Table 4.8 Percent composition of sulfonates and selectivity at 1, 2, 4, and 6 hrs

System	Reaction Time (hr)	% Di sulfonates	%Mono sulfonates	Selectivity
$1UV/O_3/O_2$	1	7.9	92.1	11.7
$2UV/O_3/O_2$	2	8.4	91.6	10.9
$4UV/O_3/O_2$	4	11.3	88.7	7.9
$6UV/O_3/O_2$	6	16.0	84.0	5.3

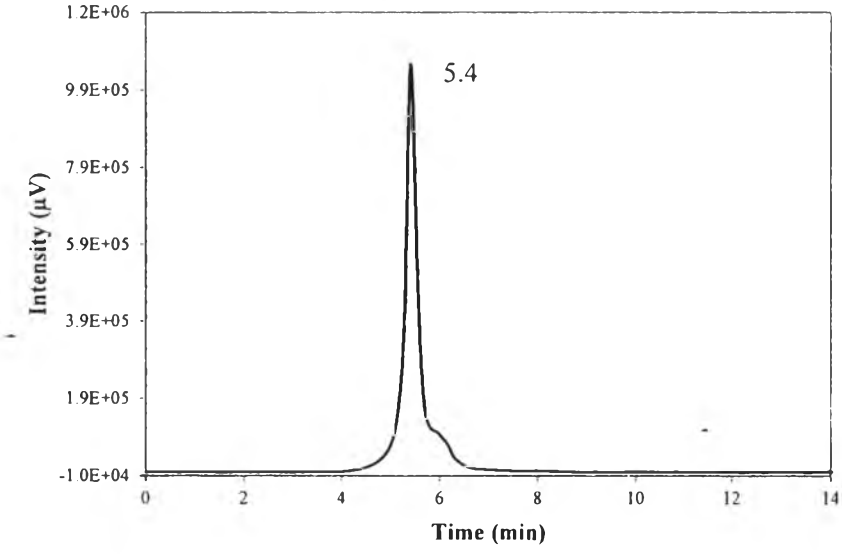

Figure 4.10 Liquid Chromatogram of α-MES C18 solution.

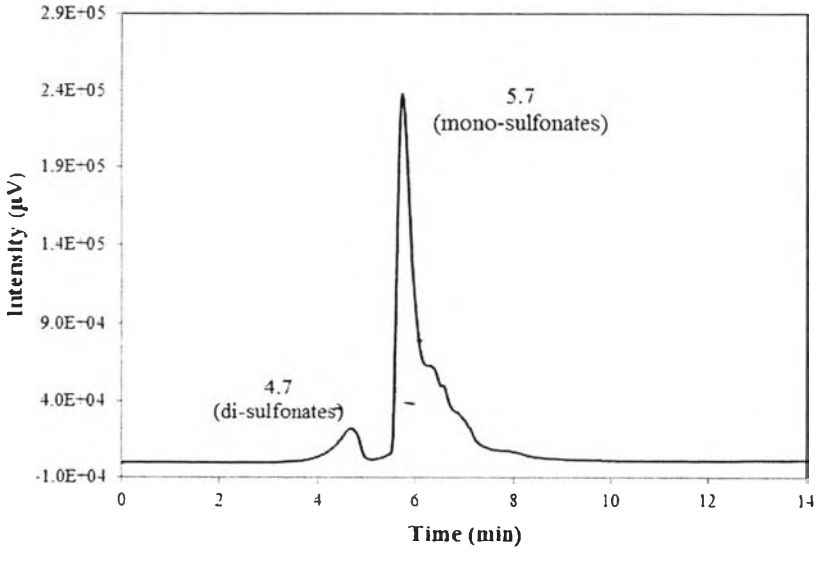

Figure 4.11 Liquid Chromatogram of MES solution of $1UV/O_3/O_2$ at 30 °C.

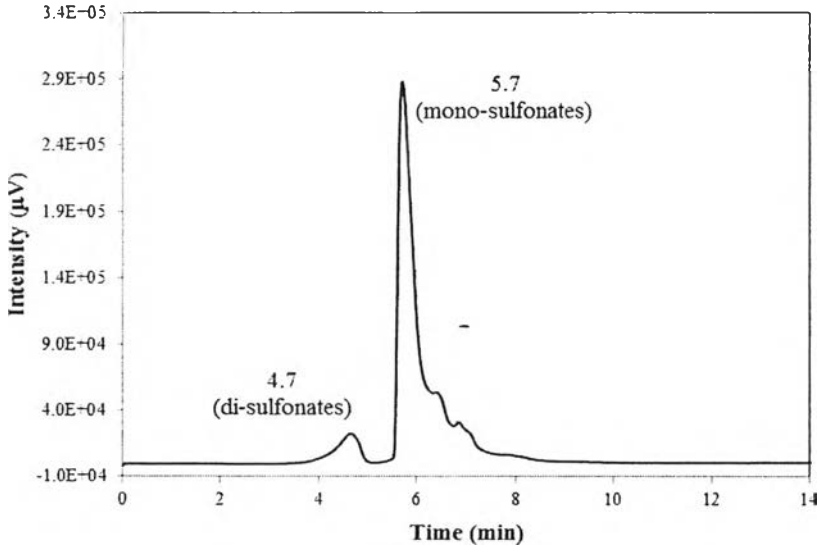

Figure 4.12 Liquid Chromatogram of MES solution of $2UV/O_3/O_2$ at 30 °C.

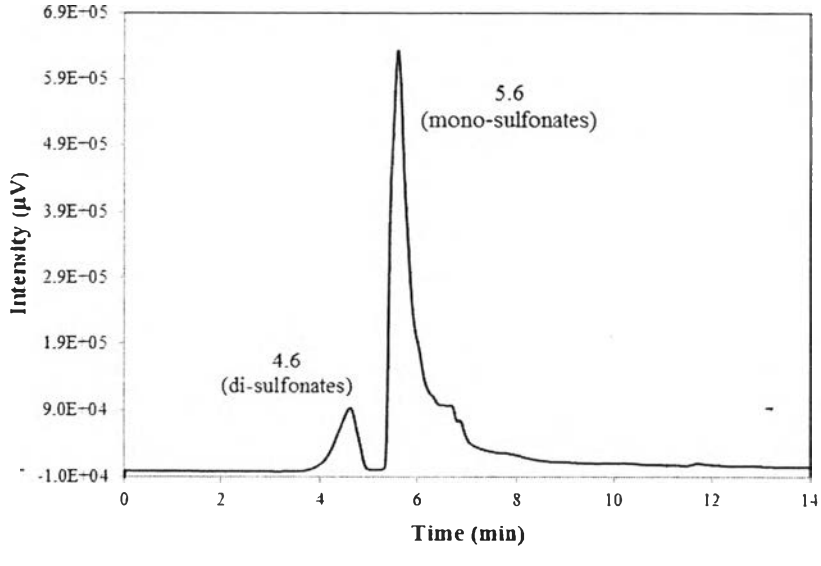

Figure 4.13 Liquid Chromatogram of MES solution of $4UV/O_3/O_2$ at 30 °C.

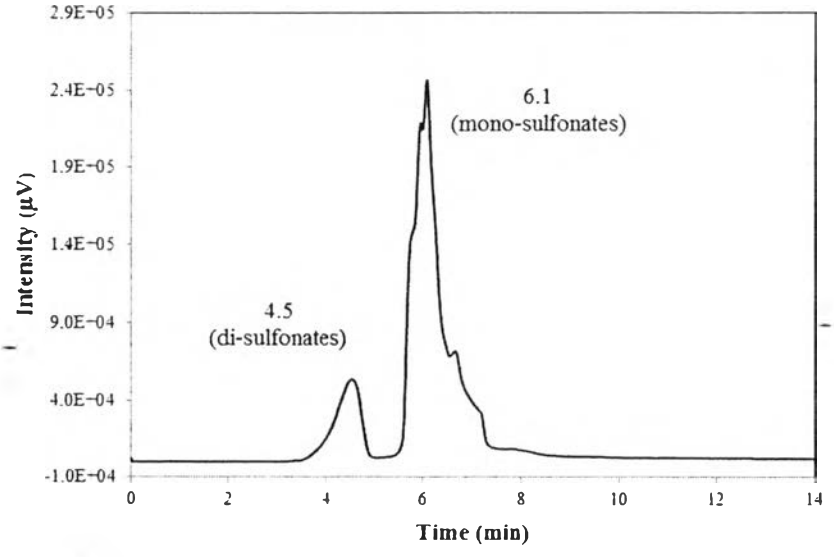

Figure 4.14 Liquid Chromatogram of MES solution of $6UV/O_3/O_2$ at 30 °C.

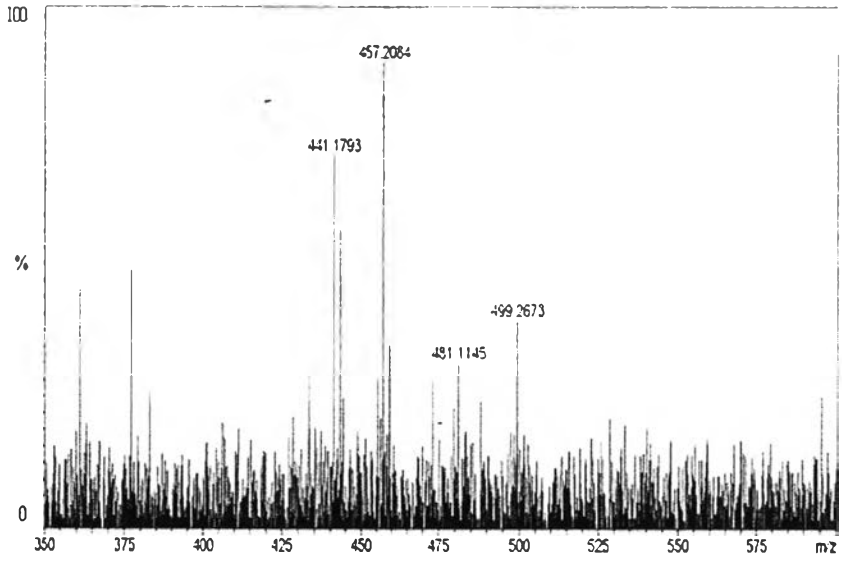

Figure 4.15 ESI-MS fingerprints of $4UV/O_3/O_2$ at ~ 4.7 min.

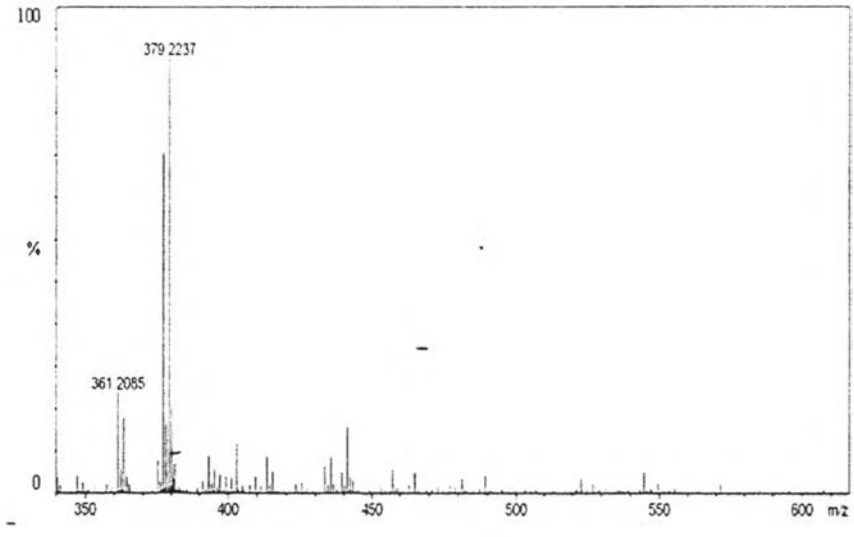

Figure 4.16 ESI-MS fingerprints of $4UV/O_3/O_2$ at ~5.7 min.

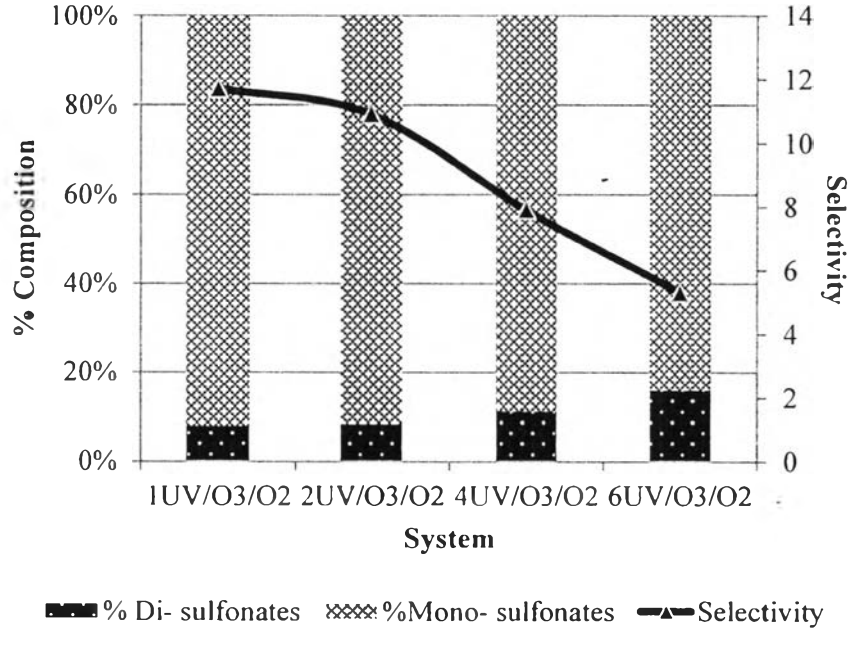

Figure 4.17 Percent composition of mono- and disulfonates and selectivity at different reaction time.